Assessment and Correction of B_1-Induced Errors in Magnetization Transfer Ratio Measurements

Stefan Ropele,[1,5]* Massimo Filippi,[2] Paola Valsasina,[2] Tijmen Korteweg,[3] Frederik Barkhof,[3] Paul S. Tofts,[4] Rebecca Samson,[4] David H. Miller,[4] and Franz Fazekas[5]

The magnetization transfer ratio (MTR) is strongly related to the field strength (B_1) of the saturation pulse. B_1 variations therefore can result in significant MTR variations and can affect histogram analysis, particularly if data from a large volume of interest are included. A multicenter study was performed to determine the typical range of B_1 errors and the corresponding MTR variations in brain tissue of healthy volunteers. Seven subjects were included at each center resulting in a total cohort of 28 subjects. Additionally, numerical simulations were done to study this relationship more generally for pulsed saturation. It could be demonstrated, both theoretically and empirically, that for typical B_1 errors there is a linear relationship between B_1 error and the corresponding MTR change. In addition, for proton density-weighted sequences, this relationship seems to be largely independent of the underlying relaxation properties.

Mean B_1 errors in the entire brain were typically in the range between -3% and -7%. Due to different coil characteristics, significant MTR differences between different scanners and sites were observed. Using a simple correction scheme that is based on a linear regression analysis between MTR and B_1 data it was possible to reduce the intersubject variation by ~50%. Furthermore, interscanner variation could be reduced such that no significant differences between scanners could be detected. The correction scheme may be useful when investigating MTR as an outcome measure in single or multicenter studies. Magn Reson Med 53:134–140, 2005. © 2004 Wiley-Liss, Inc.

Key words: magnetization transfer; white matter; B_1 mapping; multicenter study

INTRODUCTION

Magnetization transfer (MT) imaging provides an excellent opportunity to evaluate the inherent relaxation properties of heterogeneous tissues. Currently, MT is analyzed in two ways, by true quantitative MT imaging (qMTI), or alternatively, by a more relative assessment of the MT effect in terms of the MT ratio (MTR). Although only qMTI allows a detailed insight into the relaxation mechanisms (1–5), MTR mapping is more frequently performed because it can be done much faster and is technically less demanding and therefore readily available on most clinical scanners. The relative quantities that are provided by MTR mapping are also quite reproducible and comparable among subjects and repeated scans but only if the same scanner and MT sequence is used (6–8). Because of this and a high sensitivity for tissue changes MTR measurements have already been used extensively to study brain tissue abnormalities related to various diseases and also to investigate other organs. Most intriguing results have been obtained from the application in multiple sclerosis patients, where it has been possible to demonstrate abnormalities even in brain tissue that appears normal on conventional scanning, including evidence for focal tissue changes that precede lesion formation by several months (9,10). Because of the potential implication of such insights for the evaluation of drug effects, MTR imaging is increasingly used as an outcome marker in several clinical treatment trials of MS.

In these studies, the MTR is evaluated regionally in lesions and normal appearing brain tissue, and, more frequently, MTR changes are measured globally in terms of histogram analyses. A histogram analysis allows a spatially unrestricted assessment of tissue integrity while still being sensitive to small diffuse MTR changes (11). Unfortunately, variations of the MTR may not only reflect regional changes of the tissue properties (12), but also sequence and system related changes. For all these purposes it is therefore essential to minimize technically induced distortions of the apparent MTR and to correct for them to arrive at comparable results. So far this has been done primarily by the development and use of standardized protocols. The latter is of vital importance, especially in multicenter studies (7).

The B_1 field is among those factors that affect MTR measurements but it has received only limited attention in efforts to standardize MTR measurements so far. Calibration errors and nonuniformities that are caused by the coil design and by the shape and electrical properties of the investigated subject itself can result in significant local variations of the B_1 field. Continuous wave theory predicts a strong nonlinear relationship between the strength of the B_1 field and the resulting MTR (13). However, this relationship has not yet been investigated for pulsed MT saturation. Using a modern birdcage coil system, B_1 errors within a single axial slice are usually moderate ($< 5\%$), whereas more pronounced B_1 errors can be observed along the z direction. Therefore, the latter are expected to seriously influence whole-brain MTR histograms or MTR measurements in larger organs.

This study was designed to assess the extent of typical B_1 variations in brain tissue and the resulting MTR changes. For that purpose we have acquired pairs of MTR

[1]MR Research Unit, Medical University Graz, Austria.

[2]Neuroimaging Research Unit, Ospedale San Raffaele, Milano, Italy.

[3]Department of Radiology, VU Medical Centre, Amsterdam, The Netherlands.

[4]NMR Research Unit, Institute of Neurology, University College London, United Kingdom.

[5]Department of Neurology, Medical University Graz, Austria.

*Correspondence to: Stefan Ropele, MR Research Unit, Medical University Graz, Auenbruggerplatz 9, A-8036 Graz, Austria/Europe. E-mail: stefan.ropele@meduni-graz.at

Received 1 June 2004; revised 26 July 2004; accepted 11 August 2004

DOI 10.1002/mrm.20310

Published online in Wiley InterScience (www.interscience.wiley.com).

and B_1 measurements in brain tissue of healthy volunteers. To study the impact on the interscanner variability we have performed these measurement in a multicenter setting. Based on previous work (14) and on results from numerical simulations we also propose a simple B_1 correction method. Results on how this method can improve inter- and intrascanner variability are presented.

MATERIALS AND METHODS

Numerical Simulations

To correct for possible B_1 errors the exact relationship between the power of the saturation pulse and the reduction of the observable steady state magnetization has to be known. This requires the incorporation of the binary spin-bath model (BSBM), which is commonly used to study relaxation in brain tissue (15). Unfortunately, a closed solution for the steady state magnetization is given only for continuous wave saturation (13). For pulsed saturation, as commonly performed in standard MT imaging, the coupled Bloch equations have to be solved in the time domain. We therefore investigated the B_1 dependency of the steady-state magnetization by decomposing each repetition period (TR) in a period of off-resonance saturation and a period of free recovery. Free recovery was calculated with the analytical solution found by Edzes and Samulski (16). The effect of the saturation pulse was calculated by integrating the coupled Bloch equations with the fourth/fifth-order Runge–Kutta algorithm (17). The rate of saturation of the bound pool was considered a time-dependent function that regarded the shape of the saturation pulse (18). A super-Lorentzian line shape was assumed for the bound pool (19). The effect of the imaging pulse was calculated directly (i.e., by applying a rotation matrix). For simplicity, we neglected the effect of the imaging RF pulse on the bound pool magnetization. Spoiling was incorporated by setting the transverse component of the free pool magnetization at the end of each TR equal to zero. The numerical calculations were repeated for consecutive TRs until a steady state was achieved. The steady state was defined by a change of longitudinal magnetization of less than 0.01%. To obtain MTRs, the steady-state magnetization was normalized by results found for a saturation pulse with a flip angle of 0°. Simulations of B_1 errors were performed for the EURO-MT sequence (20) and, alternatively, for typical T_1-weighted MT sequences (21). We considered different kinds of brain tissue, including gray matter, white matter, and MS lesions. The relaxation properties of these tissues were taken from Ref. 2 and are summarized in Table 1.

Table 1
Fundamental parameters of the BSBM at 1.5 T used for the numerical simulations, where F is the ratio of the pool sizes, k_f is the forward transfer rate, and the subscripts f and r denote the free and restricted pools.

	Frontal white matter	MS lesion	Cortical gray matter	Caudate nucleus
F	.156	0.094	0.072	0.056
k_f (s-1)	4.5	2.7	2.4	2.2
$T_{1,f}$ (ms)	555	793	1075	1010
$T_{1,r}$ (s)	1	1	1	1
$T_{2,f}$ (ms)	34	52	56	55
$T_{2,r}$ (μs)	12	10.9	11.1	9.7

Correcting for B_1 Errors

We developed a simple B_1 correction method that is based on the idealized assumption of a linear relationship between the B_1 error and the resulting MTR error. This assumption was driven by the results of the numerical solution, which is discussed below. The relationship can be formulated as follows:

$$\mathrm{MTR}_{\mathrm{error}} = \frac{\mathrm{MTR}_{\mathrm{measured}}}{\mathrm{MTR}_{\mathrm{true}}} - 1 = kB_{1\mathrm{error}}, \qquad [1]$$

where $\mathrm{MTR}_{\mathrm{error}}$ is the relative deviation from the true MTR value and $B_{1\mathrm{error}}$ is the relative deviation of B_1 from its nominal value. We further hypothesize that the above equation holds true for each tissue which means that k is not tissue specific. Equation [1] can also be reformulated for a specific tissue such that

$$\mathrm{MTR}_{\mathrm{measured}} = \mathrm{MTR}_{\mathrm{true}} + k_{\mathrm{specific}}B_{1\mathrm{error}}, \qquad [2]$$

where k_{specific} is now a tissue specific constant that is defined by the following:

$$k_{\mathrm{specific}} = k\mathrm{MTR}_{\mathrm{true}}. \qquad [3]$$

For a given number n of voxels from a larger region of interest with corresponding MTR and B_1 values, the true MTR and the tissue-specific constant k_{specific} can simply be calculated with a linear regression according to the following:

$$\mathrm{MTR}_{\mathrm{true}} = \frac{\sum_{i=1}^{n}\mathrm{MTR}_{\mathrm{measured}}[i] - k_{\mathrm{specific}}\sum_{i=1}^{n}B_{1\mathrm{error}}[i]}{n} \qquad [4]$$

and

$$k_{\mathrm{specific}} = \frac{\sum_{i=1}^{n}B_{1\mathrm{error}}[i]\mathrm{MTR}_{\mathrm{measured}}[i] - \left(\sum_{i=1}^{n}B_{1\mathrm{error}}[i]\right)\left(\sum_{i=1}^{n}\mathrm{MTR}_{\mathrm{measured}}[i]\right)/n}{\sum_{i=1}^{n}B_{1\mathrm{error}}[i]^2 - \left(\sum_{i=1}^{n}B_{1\mathrm{error}}[i]\right)^2/n}. \qquad [5]$$

If the MTR map of heterogeneous tissue has to be corrected, the linear regression has to be performed for a homogenous subsample. For instance, segmented brain white matter could be used to evaluate the true MTR and k_{specific} according to Eqs. [4] and [5]. If both are known, k can be calculated (Eq. [3]) and the entire MTR images can be corrected pixel by pixel with the following:

$$\mathrm{MTR}_{\mathrm{true}} = \frac{\mathrm{MTR}_{\mathrm{measured}}}{kB_{1\mathrm{error}} + 1}. \quad [6]$$

Measurements

The measurements were performed on 1.5-T whole-body scanners at four different European centers, including Amsterdam, Graz, London, and Milan. Imaging was done on an Intera (Philips, Medical Systems, Best, NL), a Signa (General Electrics, Milwaukee, WI), and on two Magnetom Vision (Siemens, Erlangen, Germany). Seven healthy volunteers were imaged at each center resulting in a total cohort of 28 subjects (17 male, 11 female; mean age = 28 years). The imaging protocol included a MTR and B_1 mapping sequence, whereby both sequences had the same field of view and covered exactly the same part of the head (FOV = 250 mm, number of slices = 24, axial orientation, THK = 5 mm).

For B_1 mapping the double angle method (DAM) was applied (22). This method is based on a spin-echo or gradient-echo sequence that is performed twice with single and double values of the flip angle for the excitation pulse. Provided that longitudinal relaxation can be neglected and effects of the slice profile are only moderate, this method offers a quick and robust estimation of the B_1 error. Depending on the local capabilities to adjust the flip angle a pair of 60°/120° pulses, or alternatively a pair of 45°/90° pulses, was used. To eliminate T_1 relaxation effects a TR of at least 13 s was used. Reducing the number of phase encoding steps and, optionally, employing a fast spin-echo readout helped to shorten the scan duration. Scan parameters were adjusted individually such that the total duration for B_1 mapping was shorter than 10 min.

Magnetization transfer imaging was done with the EURO-MT sequence (20), which is based on a proton density-weighted gradient-echo sequence (matrix = 256 × 128, TR = 900 ms, TE = 12 ms, FA = 20°). The sequence was performed without and then with the application of a Gaussian-shaped saturation pulse (duration = 7.68 ms, resonance offset = 1.5 kHz, FA = 500°). One center (Philips Intera) implemented a saturation pulse that had a sinc shape instead of a Gaussian.

Data Analysis

B_1 error maps showing the percentage deviation of B_1 from its nominal value were calculated using the signal intensities obtained in the scans with the single value (I_1) and the double value of the flip angle (I_2) according to the following:

$$B_{1\mathrm{error}} = \left(\left(\arccos\frac{I_2}{2I_1} - \alpha_1 \right) / \alpha_1 \right) \times 100\%, \quad [7]$$

where the nominal flip angle α_1 was 45° or 60°. As the B_1 distribution is a rather smooth function, the maps were filtered with a 5 × 5 Gaussian kernel to reduce noise.

The MTR was calculated pixel by pixel from the following:

$$\mathrm{MTR} = \frac{M_0 - M_s}{M_0} \times 100\%, \quad [8]$$

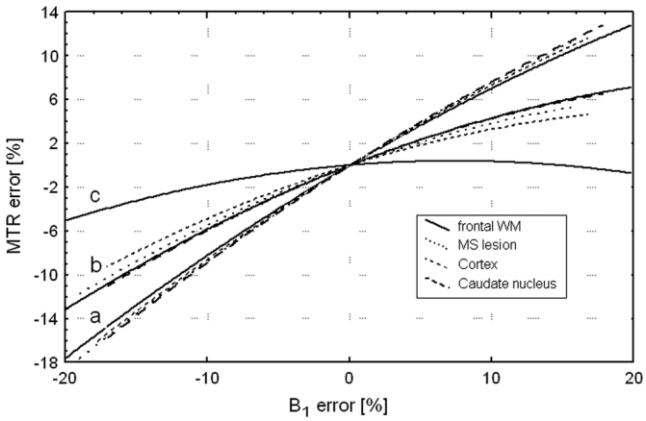

FIG. 1. Results of the numerical simulations for the EURO-MT sequence (**a**), a moderately T_1–weighted MT sequence (TR = 29 ms, FA = 12) (**b**), and for a heavily T_1 weighted MT sequence (**c**) (TR = 30 ms, FA = 25°). The B_1 error is the deviation of B_1 from its nominal value.

where M_0 and M_s are the signal intensities obtained without and with the application of the saturation pulse, respectively. To find the non-tissue-specific relationship between MTR error and B_1 error we first determined the true MTR and k_{specific} for brain white matter according to Eqs. [4] and [5]. Segmentation of supratentorial white matter was done on the MT-weighted images with a few standard image-processing steps. First, brain was extracted using a brain extraction tool (BET, fMRIB Oxford, England). Then a white matter mask was produced by applying a lower and upper signal intensity threshold. Finally, the binary mask was eroded by 1 pixel to reduce possible partial volume effects with gray matter or cerebrospinal fluid. After k was calculated, the entire MTR map was corrected in accordance with Eq. [6].

To evaluate the benefit of the correction scheme we first performed comparative region-of-interest measurements. Two circular regions of interest with a diameter of approximately 1 cm were placed in the left and right frontal white matter and the mean value of both regions was taken for the analysis. Additionally, the peak position of whole-brain histograms and the mean MTR of segmented white matter were determined for corrected and uncorrected MTR maps.

RESULTS

The numerical simulations supported our hypothesis of a linear relationship between B_1 error and corresponding MTR error. As a proof of Eq. [1] these simulations also confirmed that this correlation is largely tissue independent. Some representative results of the simulations are shown in Fig. 1. Interestingly, the strongest B_1 sensitivity can be observed for proton density-weighted sequences, where a B_1 error of 10% is reflected by approximately a 9% MTR change. Although moderately T_1-weighted MT sequences have a lower B_1 sensitivity, the MTR produced by heavily T_1-weighted sequences is not sensitive to B_1 errors. However, as apparent from Fig. 1, the linearity and

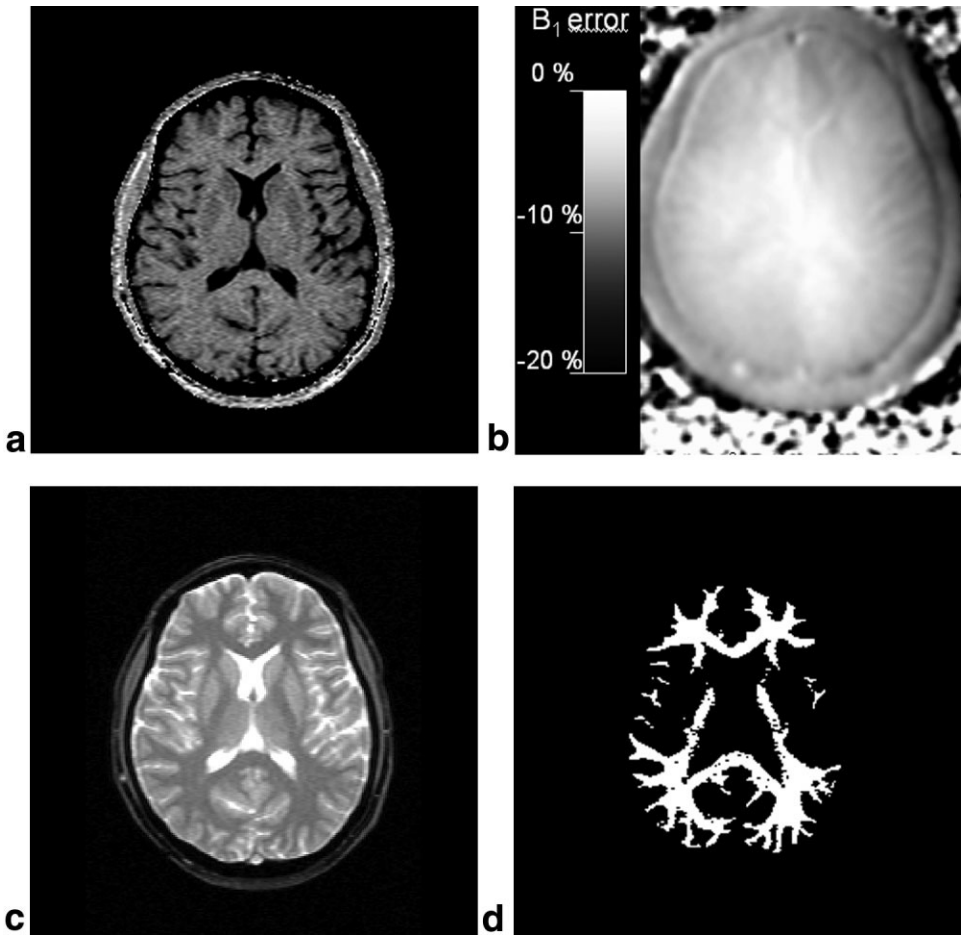

FIG. 2. Representative data set from a healthy volunteer showing (**a**) MTR map, (**b**) B_1 map, (**c**) MT weighted scan (M_S), and (**d**) white matter mask.

the tissue independency of k gets lost with stronger T_1 weighting.

Figure 2 shows a representative data set from a volunteer, including the MTR and B_1 map, the MT weighted scan, and the corresponding white matter mask.

We found mean B_1 errors over the entire brain to be typically in the range between -3% and -7%, whereas the maximum B_1 variation within the brain was up to ± 20% in many cases. We also observed scanner specific B_1 distribution patterns, which indicates that coil design may play a dominant role.

Figure 3 illustrates the result of a linear regression analysis that was performed for segmented white matter. Considering the limited accuracy of the B_1 mapping method, the non-tissue-specific constant k derived from this analysis ($k = 0.79$) was in good agreement with the results from numerical simulations ($k \approx 0.9$). In a few selected volunteers B_1 errors were also simulated by changing the nom-

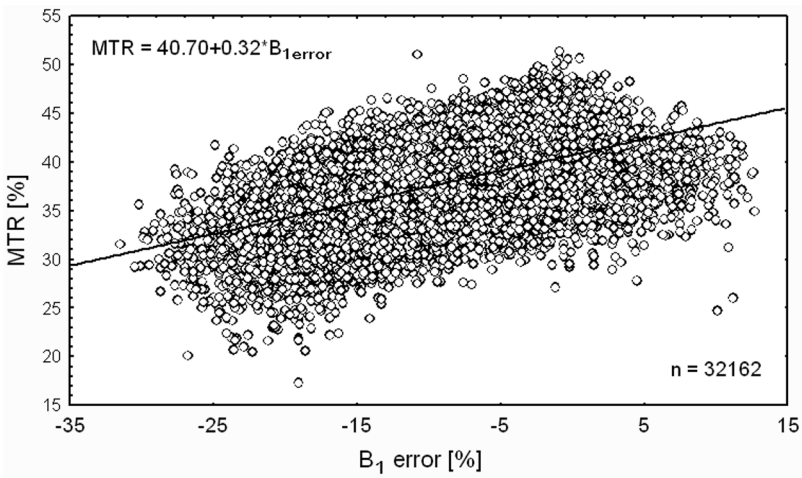

FIG. 3. Correlation between the B_1 error and the corresponding MTR in segmented white matter of a single volunteer.

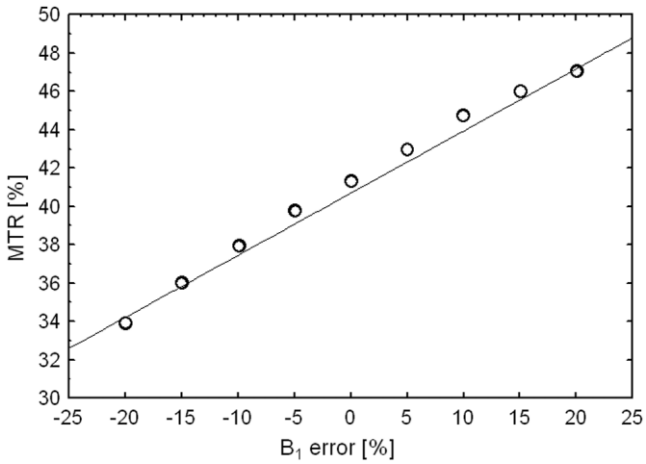

FIG. 4. MTR obtained in frontal white matter as a function of B_1 error (circle). B_1 variation was achieved by varying the flip angle of the MT pulse in steps of 25°. The solid line represents the slope found by a linear regression analysis in the same volunteer (Fig. 3).

inal MT pulse flip angle in 25° steps. We found a good agreement between the slope obtained from the linear regression analysis and the slope obtained independently by the experimental B_1 variation (Fig. 4).

The application of the correction scheme resulted in remarkable shifts of the MTR histograms toward higher MTR values. In a few individuals we could also observe a reduction of the histogram dispersion and an increase of the peak height (Fig. 5).

The results of the MTR analysis in frontal white matter, segmented white matter, and whole brain are summarized in Table 2. Using a nonparametric Kruskal–Wallis one-way ANOVA we found significant MTR differences across different sites ($P \leq 0.008$) before B_1 correction. After B_1 correction the intersubject variability was remarkably reduced. Although the intersubject variability for frontal white matter could only be slightly reduced, a reduction in variation of approximately 50% could be achieved in whole brain and segmented white matter. Additionally, the B_1 correction method reduced the inter scanner variation such that the ANOVA did no longer show any significant differences. Centre 4 was excluded from the ANOVA because a different MT pulse had been used there.

DISCUSSION

In an overall attempt to make MTR measurements comparable both on an individual basis as well as between different investigational sites this study explored the magnitude of data distortion from B_1 nonuniformities and B_1 calibration errors and attempts to correct for such influence. The nonuniformity of the transmitter coil is a well-known source of MTR variations (6,23). Although the use of the main body coil for MT saturation can improve the situation (24), still significant variations may occur. In this work we have demonstrated that in brain tissue B_1 errors up to 20% can occur. Importantly, there appears to be a linear relationship between B_1 errors and the resulting MTR variations based on theoretical considerations and our experimental findings. This was partly unexpected as continuous wave theory predicts a nonlinear relationship. The expected nonlinearity and tissue dependency were probably also the reasons why no attempts to correct for the B_1 error have been made so far. Fortunately, the linear relationship makes it possible to employ a simple correction scheme that is based on a linear regression analysis.

Interestingly, the numerical simulations suggest only a limited sensitivity to B_1 errors for heavily T_1-weighted MT scans. A possible explanation for this phenomenon is that MT has only a limited contribution to relaxation when both spin pools approach full saturation. A stronger B_1 field will result in a higher flip angle of the imaging pulse and therefore in a higher saturation of the water protons. In parallel, the higher flip angle of the MT pulse will result in a stronger saturation of the bound protons. That means that a stronger B_1 field produces a stronger saturation of the bound pool but simultaneously reduces the sensitivity of the sequence for saturation transfer. The effects seem to counteract each other in heavily T_1-weighted sequences in such a way that the overall B_1 sensitivity is only small.

We used the DAM method for B_1 mapping in this study because it is simple and robust and can be employed with slice-selective pulses. With this method errors in the B_1

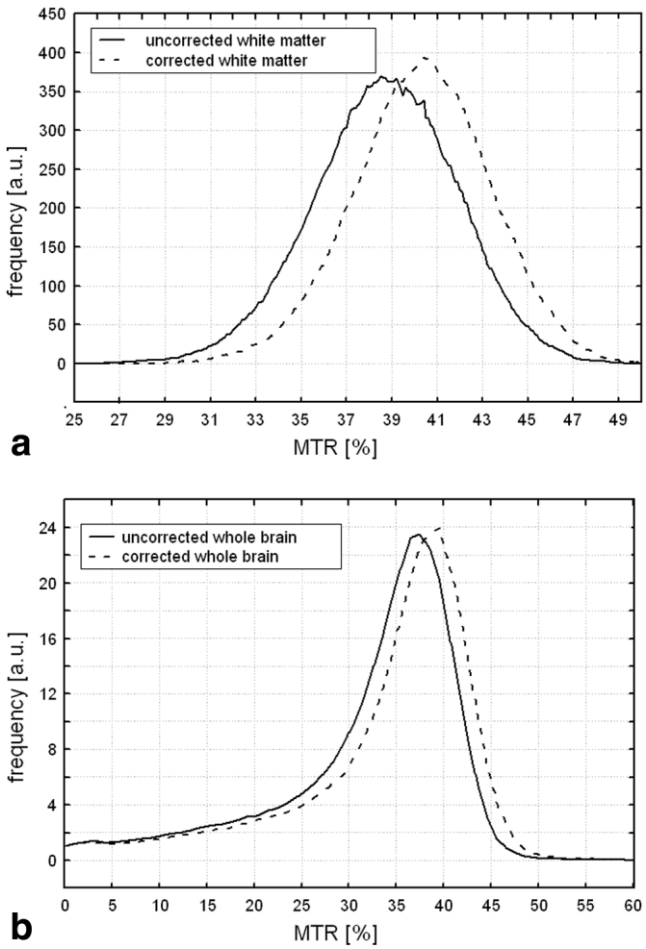

FIG. 5. Effect of the B_1 correction method on the white matter histogram (**a**) and normalized whole brain histogram (**b**) from a single subject.

Table 2
Results of the MTR analysis before and after B_1 correction.

	Segmented WM mean MTR (SD)		Frontal WM mean MTR (SD)		Whole brain histogram peak position (SD)	
	Uncorrected	Corrected	Uncorrected	Corrected	Uncorrected	Corrected
Centre 1	38.9 (0.45)	41.3 (0.33)	38.9 (0.30)	41.2 (0.28)	36.9 (0.41)	39.1 (0.34)
Centre 2	39.0 (1.05)	41.2 (0.43)	41.4 (1.35)	42.7 (1.34)	37.9 (0.89)	39.5 (0.39)
Centre 3	40.0 (0.77)	41.0 (0.46)	40.8 (1.27)	41.6 (0.96)	38.4 (0.86)	39.0 (0.39)
Centre 4[a]	42.5 (0.85)	43.7 (0.51)	42.8 (1.25)	44.2 (0.79)	41.3 (0.87)	42.6 (0.41)
Mean[b]	39.3 (0.89)	41.2 (0.36)	40.5 (1.50)	41.9 (1.15)	37.8 (0.96)	39.2 (0.43)

Note. MTR values and standard deviation (SD) are given in percentage units.
[a]A non-Gaussian MT pulse was used.
[b]Centre 4 was not considered.

calculation can be caused by T_1 relaxation effects and nonideal slice profiles and, for higher RF power, from nonlinearities of the RF amplifier. As a proof of the accuracy of this method we found a good agreement between the measured B_1 error and experimentally induced errors in a few selected cases (Fig. 4). However, it is important to note that a high accuracy of the B_1 mapping method is not a prerequisite for the regression analysis. Inaccurate B_1 values will only affect the slope in the regression analysis. The most important prerequisite is that the B_1 error map scales linearly with the true B_1 error. This also means that a B_1-weighted sequence could be used instead of an absolute technique, which could help to improve the applicability of suggested correction scheme in a clinical setting. Further efforts will have to focus on the selection and optimization of such a sequence.

With our correction scheme we could significantly improve intersubject and intersite variability. After B_1 correction the variation of the mean MTR between different scanners was within the mean intersubject variability. This implies that MTR differences that are usually observed between sites are mainly due to B_1 effects. The capability to reduce intersubject variability and to minimize center specific effects should have great impact on multicenter MTR studies, because it will improve statistical power.

Some limitations and directions of future research should also be noted. All simulations and measurements in this work were done with shaped off-resonance MT pulses. Therefore our results generally are not valid for binomial pulses, which can also be used for MT saturation (25). Further work is needed to investigate the B_1 sensitivity of binomial saturation schemes. Future work will also have to focus on the question if B_1 mapping based on a phantom provides results that are equivalent to B_1 mapping in vivo. Some T_1 relaxation studies have used an oil phantom to produce a reference B_1 map for T_1 correction (26). This approach is based on the assumption that the coil load and dielectrical properties of an individual head do not deviate much from those of the phantom. In addition it is assumed that the coil design is the most dominant factor that determines the B_1 distribution. The latter is also supported by our experimental data, where we have observed strong coil related B_1 profiles. However, this issue needs further clarification, in particular for higher field strength.

CONCLUSION

B_1 variations appear to be a major source for intersubject and interscanner variability commonly observed in MTR measurements. We have shown, both theoretically and experimentally, that for proton density-weighted MT sequences there exists a linear relationship between B_1 error and MTR error. This relationship is largely independent of the relaxation properties of the underlying tissue. With a linear regression analysis it is possible to eliminate the influence of B_1 errors if absolute or relative B_1 maps are available and thus to significantly increase the comparability of MTR values obtained.

ACKNOWLEDGMENTS

The authors are members of the MAGNIMS network, which is a group of European clinicians and scientists with an interest in performing collaborative studies using MR methods in MS. The network is independent of any other organization and is run by a Steering Committee whose members are D. Miller, London (co-chair), M. Filippi (Milan, co-chair), F. Barkhof (Amsterdam), F. Fazekas (Graz), L. Kappos (Basel), X. Montalban (Barcelona), C. Polman (Amsterdam), A. Thompson (London), and T. Yousry (London). We thank the Steering Committee for its support. This research was also supported by a grant from the Austrian Science Foundation (grant P-15158).

REFERENCES

1. Gochberg DF, Kennan RP, Robson MD, Gore JC. Quantitative imaging of magnetization transfer using multiple selective pulses. Magn Reson Med 1999;41:1065–1072.
2. Sled JG, Pike GB. Quantitative imaging of magnetization transfer exchange and relaxation properties in vivo using MRI. Magn Reson Med 2001;46:923–931.
3. Yarnykh VL. Pulsed *Z*-spectroscopic imaging of cross-relaxation parameters in tissues for human MRI: theory and clinical applications. Magn Reson Med 2002;47:929–939.
4. Ramani A, Dalton C, Miller DH, Tofts PS, Barker GJ. Precise estimate of fundamental in-vivo MT parameters in human brain in clinically feasible times. Magn Reson Imaging 2002;20:721–731.
5. Ropele S, Seifert T, Enzinger C, Fazekas F. Method for quantitative imaging of the macromolecular ^{1}H fraction in tissues. Magn Reson Med 2003;49:864–871.
6. Silver NC, Barker GJ, Miller DH. Standardization of magnetization transfer imaging for multicenter studies. Neurology 1999;53(Suppl 3): 33–39.

7. Berry I, Barker GJ, Barkhof F, Campi A, Dousset V, Franconi JM, Gass A, Schreiber W, Miller DH, Tofts PS. A multicenter measurement of magnetization transfer ratio in normal white matter. J Magn Reson Imaging 1999;9:441–446.
8. Sormani MP, Iannucci G, Rocca MA, Mastronardo G, Cercignani M, Minicucci L, Filippi M. Reproducibility of magnetization transfer ratio histogram-derived measures of the brain in healthy volunteers. Am J Neuroradiol 2000;21:133–136.
9. Filippi M, Rocca M, Martino G, Horsfield MA, Comi G. Magnetization transfer changes in the normal appearing white matter precede the appearance of enhancing lesions in patients with multiple sclerosis. Ann Neurol 1998;43:809–814.
10. Fazekas F, Ropele S, Enzinger C, Seifert T, Strasser-Fuchs S. Quantitative magnetization transfer imaging of pre-lesional white-matter changes in multiple sclerosis. Mult Scler 2002;8:479–484.
11. Van Buchem M, McGowan JC, Kolson DL, Polansky M, Grossman RI. Quantitative volumetric magnetization transfer analysis in multiple sclerosis: estimation of the macroscopic and microscopic disease burden. Magn Reson Med 1996;36:632–636.
12. Sled JG, Levesque I, Santos AC, Francis SJ, Narayanan S, Brass SD, Arnold DL, Pike GB. Regional variations in normal brain shown by quantitative magnetization transfer imaging. Magn Reson Med 2004;51: 299–303.
13. Henkelman RM, Huang X, Xiang QS, Stanisz GJ, Swanson SD, Bronskill MJ. Quantitative interpretation of magnetization transfer. Magn Reson Med 1993;29:759–766.
14. Samson RS, Wheeler-Kingshott CA, Tozer DJ, Tofts PS. A simple correction for B1 inhomogeneities in MTR measurements. In: Proceedings of the 12th Annual Meeting of ISMRM, Kyoto, Japan, 2004. p 2703.
15. Wolff SD, Balaban RS. Magnetization transfer contrast (MTC) and tissue water proton relaxation in vivo. Magn Reson Med 1989;10(1):135–144.
16. Edzes HT, Samulski ET. The measurement of cross-relaxation effects in the proton NMR spin-lattice relaxation of water in biological systems: hydrated collagen and muscle. J Magn Reson 1978;31:207–229.
17. Press WH, Flannery BP, Teukolsky SA, Vetterling WT. Numerical recipes in C: the art of scientific computing, 2nd ed. Cambridge: Cambridge University Press; 1992. p 1020.
18. Graham SJ, Henkelman RM. Understanding pulsed magnetization transfer. J Magn Reson Imaging 1997;7:903–912.
19. Morrison C, Henkelman RM. A model for magnetization transfer in tissues. Magn Reson Med 1995;33:475–482.
20. Barker GJ, Schreiber W, Gass A et al. Standardising magnetisation transfer ratio measurements between MR scanners from different manufacturers. In: Proceedings of the 5th Annual Meeting of ISMRM, Vancouver, Canada, 1997. p 1556.
21. Kabani NJ, Sled JG, Shuper A, Chertkow H. Regional magnetization transfer ratio changes in mild cognitive impairment. Magn Reson Med 2002;47:143–148.
22. Stollberger R, Wach P. Imaging of the active B1 field in vivo. Magn Reson Med 1996;35:246–251.
23. Silver NC, Barker GJ, Gass A, Schreiber W, Miller DH, Tofts PS. Magnetisation transfer measurements of the brain depend on region of interest position within headcoil. In: Proceedings of the 5th Annual Meeting of ISMRM, Vancouver, Canada, 1997. p 662.
24. Tofts PS, Yeung R, Barker GJ. Improvement in MTR histogram multicentre performance using a receive-only head coil: the PLUMB plot. In: Proceedings of the 10th Annual Meeting of ISMRM, Honolulu, USA, 2002. p 2283.
25. Pachot-Clouard M, Darrasse L. Optimization of T2-selective binomial pulses for magnetization transfer. Magn Reson Med 1995;34:462–469.
26. Parker GJ, Barker GJ, Tofts PS. Accurate multislice gradient echo T(1) measurement in the presence of non-ideal RF pulse shape and RF field nonuniformity. Magn Reson Med 2001;45:838–845.